applied sciences

MDPI

Article

Study of Dynamic Response Characteristics of the Wind Turbine Based on Measured Power Spectrum in the Eyewall Region of Typhoons

Ran Han, Long Wang *, Tongguang Wang, Zhiteng Gao and Jianghai Wu

Jiangsu Key Laboratory of Hi-Tech Research for Wind Turbine Design, Nanjing University of Aeronautics and Astronautics, Nanjing 210016, China; hanran@nuaa.edu.cn (R.H.); tgwang@nuaa.edu.cn (T.W.); gzt200361@163.com (Z.G.); jianghaiwu@nuaa.edu.cn (J.W.)

* Correspondence: longwang@nuaa.edu.cn; Tel.: +86-139-5204-8390

Received: 6 May 2019; Accepted: 4 June 2019; Published: 12 June 2019

Abstract: The present research envisages a method for calculating the dynamic responses of the wind turbines under typhoon. The measured power spectrum and inverse Fourier transform are used to generate the fluctuating wind field in the eyewall of the typhoon. Based on the beam theory, the unsteady aerodynamic model and the wind turbine dynamic model are coupled to calculate the dynamic response. Furthermore, using this method, the aeroelastic responses of a 6 MW wind turbine at different yaw angles are studied, and a 2 MW wind turbine are also calculated to verify the applicability of the results for different sizes of wind turbines. The results show that the turbulence characteristics of the fluctuating wind simulated by the proposed method is in good agreement with the actual measurement. Compared with the results simulated by the recommended power spectrum like the Kaimal spectrum, the energy distribution and variation characteristics simulated by the proposed method represent the real typhoon in a superior manner. It is found that the blade vibrates most violently at the inflow yaw angle of 30 degrees under the coupled effect of the aerodynamic, inertial and structural loads. In addition, the load on the tower exceeds the design limit values at the yaw angles of both 30 degrees and 120 degrees.

Keywords: typhoon; wind turbine; measured power spectrum; numerical simulation; dynamic response; yaw angle

1. Introduction

Typhoons are a kind of extreme weather with a large-scale vorticity system. Based on the structural characteristics of typhoon, it is usually divided into three parts: wind eye region, eye wall region and outer gale region. The eye area of a typhoon exhibits the subsidence airflow and the speed of the wind is so low that it can be ignored. The characteristics of wind field in the outer gale region are similar to the normal situation, where the destructiveness is small. However, there are extreme gusts, turbulent fluctuations and sudden changes of wind direction in the eye wall region that lead serious hazards to the large offshore wind turbines [1–4]. The schematic of the physical phenomena is shown in Figure 1. By the observations of strong typhoon such as "Hagupit" and "Parrot", it is found that there exist more extreme gusts during the 10-min observation of typhoon than the normal wind, the wind speed can change 17.6 m/s in 3 s, and the wind direction can change 28 degrees [5] in 6 s. Furthermore, the three-dimensional turbulence is so extreme that the turbulence intensity in the longitudinal direction can reach 18% (the reference value of IEC61400-1 standard is 12% [6]), which greatly exceeds the prescribed limit value by the design standard.

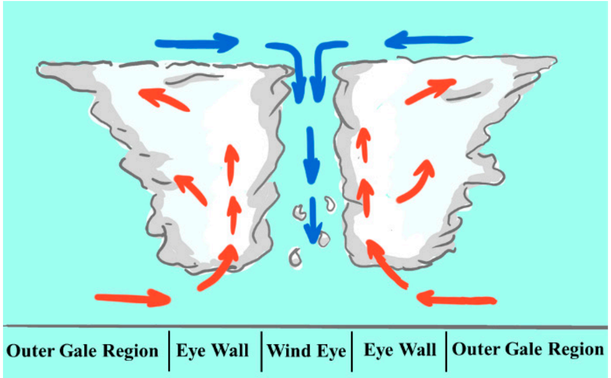

Figure 1. The schematic of typhoon structure.

To study the dynamic response characteristics of the wind turbines under typhoons, an involvement of the complex coupling of multiple models and methods from different disciplines is needed. A lot of research has been done that mainly focused on the models calculating the aerodynamic loads [7–12], the dynamic models calculating the effect on the complete wind turbine [13–15] and aeroelastic analysis methods [16–18]. However, there are a few studies that compare the reliability and accuracy of a simulating typhoon wind field. Han [19] measured the whole process of typhoon from landing to departure. It is found that the turbulence intensity and turbulence integral scale at different times are significantly different. The power spectrum fitted by the measured data is quite different from the Von Karman spectrum in the low frequency part. According to the measured data of typhoon Usagi, Chen [20–22] fitted the wind profile to construct the wind field of typhoon using solely the average speed, and carried out the static analysis of wind turbine. In other reports, the fluctuating wind field was simulated by combining the power spectrum and the wind profile [23,24]. The spectrums used in these simulations are fitted according to the data of the normal wind. Lian [25] combined the typhoon profiles with the CFD (Computational Fluid Dynamics) method to improve the accuracy of aerodynamic calculation of wind turbines, but the power spectrum of the typhoon was not used when the turbulence characteristics of far-field boundary are input, and the calculation amount of this method is huge. Based on the above research findings in literature, there is significant room for the improvement in accuracy of the typhoon fluctuating wind field simulation.

On the other hand, the wind direction in the eyewall region of the typhoon varies dramatically [26]. Although the wind turbine would be shut down in typhoons, and the yaw system would still be in working condition so as to adjust the position of the rotor to keep it against the incoming flow, there still exists a delay for a certain period of time (typically, 10 min) due to the statistical time consumed for the wind direction changes [27]. Therefore, the wind turbine may run for a long time at large yaw angle under typhoon, which will bring serious hazards in terms of structural safety of the wind turbine blades and towers. At present, most of the research working on the impact of yaw on wind turbines focuses on the aerodynamic performance affected by the yaw-induced inclined wake on blades [28–30]. There are a few further studies on the vibration response and structural damage caused by yawing of wind turbines. It was found that, when the deflection of the incoming flow reached 30 degrees and 40 degrees, the thrust of the wind turbine changed by 17% and 44%, respectively [31,32]. When the yaw angle was between 40 and 50 degrees, the wind turbine blades stalled. The vibration response analysis of the wind turbine under various conditions was carried out based on experiments, which showed that the existence of yaw angle increased the vibration of the blades at low natural frequencies [33]. Through the structural health monitoring [34,35], it was found that the yaw angle affected the dynamic response of the wind turbine blades in a frequency domain that changed to lower frequency. Once the wind turbine exhibited a significant yaw in extreme weather, it would lead to an increase in the tower stress with a risk of being damaged.

In view of the shortcomings of the current research, this paper combines the measured data of typhoon eye wall region with the power spectrum method to simulate the fluctuating wind with typhoon characteristics, and combines them with the aerodynamic and dynamic models of the wind turbines to study the aeroelastic response characteristics of wind turbines with different yaw angles.

2. Methods

The research of dynamic simulation of wind turbine under typhoon mainly includes three parts: simulation of typhoon fluctuating wind, modeling of wind turbine and aeroelastic response analysis. The whole framework is shown in Figure 2. Combined with the inverse Fourier transform method, the fluctuating wind is simulated by the power spectrum to record from the measured data of typhoon. A 6 MW wind turbine is modeled, the aerodynamic loads and aeroelastic are calculated by the blade element momentum and multibody dynamics. The aeroelastic responses and ultimate loads of the wind turbine at different inflow angles of typhoon are studied.

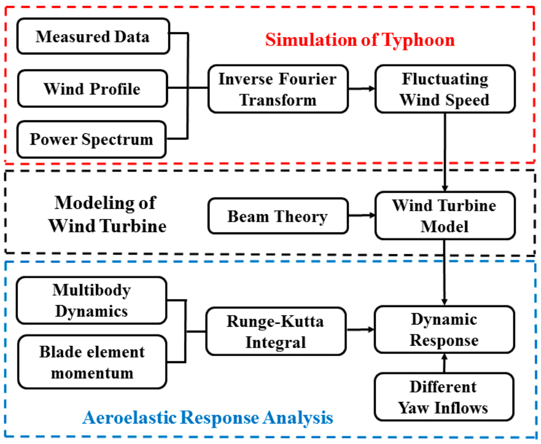

Figure 2. Block diagram structure of the analysis of wind turbine in typhoons.

According to the recorded data of the typhoon "Hagupit" [36], the wind speed in different regions of typhoons changes notably. From the typhoon gale region to the eye wall region and then to the typhoon center, the wind speed increases first and later decreases, respectively. After the typhoon center, the wind direction changes up to 180 degrees, so as to form a circular structure. The wind speed of the whole typhoon presents the distribution like the letter "M". Different researchers have fitted the typhoon measured data, of which the most suitable results are selected in relation with the characteristics of the eye wall region. The index of wind profile is 0.158, which is substituted in the index model listed as Equation (1):

$$v = v_0\left(\frac{h}{h_0}\right)^{\alpha}. \tag{1}$$

The simulation of the typhoon needs a combined mean and fluctuating wind speed, and the spectral method is usually the general method to simulate the fluctuating wind distribution. Wind power spectral density (PSD) is the important parameter for describing and simulating in this part, which characterizes the energy distribution of the turbulence in different frequency ranges. At present, most of the studies taking into account these factors in wind energy usually adopt the Kaimal spectrum or Von Karman spectrum recommended in various standards [37], which are not combined with the measured data under the real typhoon environment. Obviously, the fluctuation characteristics of typhoon are quite different from that of the normal strong wind, so the spectral function in the specification is not applicable. In order to ensure the accuracy of the simulated fluctuating wind to represent the typhoon, the determination of the parameters in the fluctuating power spectrum should be based on the measured data from the strong typhoon as described above. Referring to the records and analysis of the fluctuating data of typhoon "Hagupit" from earlier reports [38,39], the eyewall region of typhoon "Hagupit" is obtained based on the framework of the Moning–Obukhov similarity theory and the homogeneous isotropic turbulence theory. The power spectrum functions in three directions are shown in Equation (2):

$$\begin{cases} \frac{nS_u(n)}{u_*^2} = \frac{0.647f}{0.029+1.808f^{5/3}} \\ \frac{nS_v(n)}{u_*^2} = \frac{0.258f}{0.019+1.8f^{5/3}} \\ \frac{nS_w(n)}{u_*^2} = \frac{0.224f}{0.148+2.869f^{5/3}} \end{cases} . \tag{2}$$

In order to obtain the inflow conditions of typhoon for subsequent dynamic calculation, it is essential to convert the fitted power spectral density function to the frequency domain to simulate the fluctuating wind speed during the whole period according to the stationary Gauss process. Since the measured power spectrum of the typhoon has been fixed above in this paper, the inverse Fourier transform method [40] is chosen to realize the situation. This method can simulate the ideal wind field similar to the measured data with a high accuracy. The basic theory is as follows:

Given the known fluctuating power spectrum $S(n)$ and simulation time T, the Fourier amplitude spectrum $F(n)$ can be calculated from the following formula because of the ergodicity of the process of fluctuating wind speed from Equation (3) as:

$$F(n) = \sqrt{T \cdot S(n)}. \tag{3}$$

After inverse discrete Fourier transform of complex sequence $F(n)$, the real part represents the fluctuating wind in Equation (4) as:

$$v(t) = real[IDFT(\sqrt{T \cdot S(n)})]. \tag{4}$$

Considering that the wind turbine blade is a flexible structure with a large slenderness ratio, the spatial correlation of each simulation node in the wind field should be taken into account while generating fluctuating wind speed. The expression of the correlation function is shown in Equation (5) [41]:

$$coh(i,k) = e^{(-\frac{|z_i - z_k|}{L_z})}. \tag{5}$$

The aerodynamic and dynamic characteristics of the wind turbine are analyzed using the commercial software GH-Bladed [42]. The unsteady blade element momentum theory is used in the aerodynamic calculation, adding the dynamic inflow and stall models for the unsteady aerodynamic effects. The expression of structural response is based on the multibody dynamics. The floquet analysis method is used to determine the modal characteristics of the periodic systems. Different coordinate systems are established for the main components of wind turbines, so that the modal characteristics of each component can be calculated independently. The motion equation is established at the period of response analysis. The differential equation is time-advanced by using fourth-order Runge–Kutta numerical integration method with variable step size. Finally, the coupling of aerodynamics and structure is obtained by solving the equation and getting the response of each mode. It should be noted that, although there is a module of wind modeling in GH-Bladed, the software can only generate gusts and turbulent winds under normal conditions, but not inflows with typhoon structure characteristics. Therefore, the typhoon generation codes are developed in this study and are incorporated into the GH-Bladed to obtain the wind turbine structural dynamic response in typhoons.

3. Results and Analysis

3.1. Wind Turbine Model

Based on the beam theory, a commercial 6 MW offshore wind turbine is modeled. The specific model parameters are given in Table 1. The first and second natural frequency of blades and the tower are calculated. The total simulation area of the typhoon is 200 m × 200 m, which is discretized into 256 nodes, covering the whole rotor, as shown in Figure 3. The position and direction of the blades are also indicated with the state of parking. In the process of dynamic calculation, the flow direction facing the rotor is 0 degrees, clockwise, it is positive and counterclockwise, it was negative. In this paper, the aeroelastic response of the complete wind turbine is calculated in seven cases at yaw angles of 0, 30, 60, 90, 120, 150 and 180 degrees.

Table 1. 6 MW wind turbine parameters.

Parameter	Value	Parameter	Value
Rated speed	10.5 m/s	Hub height	100 m
Number of blades	3	Blade length	78 m
Diameter of rotor	160.7 m	Tip prebending	4.5 m
First-order natural frequency (out of plane)	0.438 Hz	First-order natural frequency (in plane)	0.826 Hz
Second-order natural frequency (out of plane)	1.364 Hz	Second-order natural frequency (in plane)	2.565 Hz
First-order natural frequency of tower	0.217 Hz	Second-order natural Frequency of tower	1.321 Hz

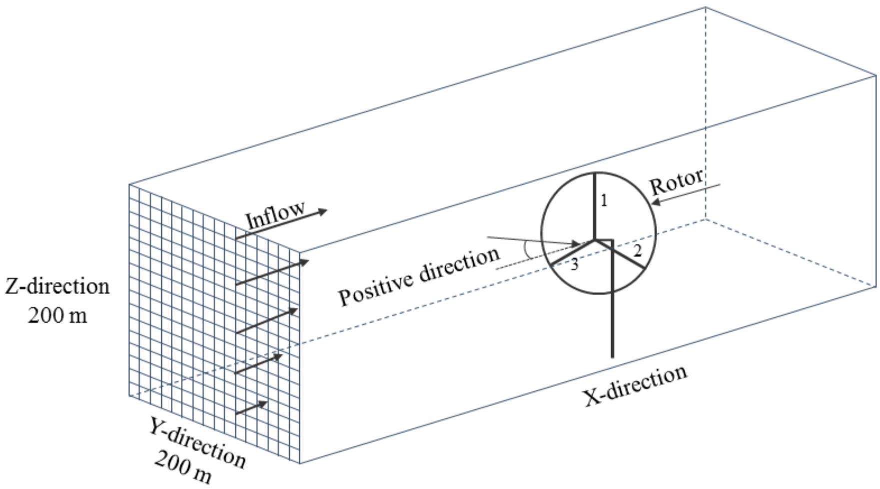

Figure 3. Calculation zone and node partition.

3.2. Analysis of Wind Characteristics

Figure 4 shows the comparison of the fluctuating power spectral intensities in the three directions between the simulated and measured results. The generated spectrum fluctuates around the target spectrum, and there is no large deviation, demonstrating that the turbulence characteristics of the simulated fluctuating wind are in line with the measured actual typhoon. In addition, the longitudinal fluctuating energy is higher than the other directions, and the vertical energy is the lowest, which corresponds to the fluctuating wind speed in the three directions. In addition, the fluctuating wind using the Kaimal spectrum and Von Karman spectrum that are commonly used in the specification were also simulated, and compared with the results of the measured typhoon spectrum. At the hub height of the wind turbine, the turbulence intensities of the three fluctuating wind were 10.83%, 10.35 and 13.89%, respectively. In order to quantify the error of the numerical results, Table 2 shows the comparison of the turbulence intensities in three directions between the simulated and the measured results at the height of the anemometer. The results simulated by the proposed method in this paper are in good agreement with the measured ones. The most important longitudinal error for wind turbine dynamics simulation is only 1.7%, and the turbulent fluctuation is higher than the recommended spectrum in the standards; this difference reflects the particularity of typhoon. Figure 5 shows the fluctuating wind speed in three directions at the hub height of the wind turbine. The longitudinal inflow fluctuation reaches a value of 36.73 m/s. The horizontal and vertical fluctuation amplitudes are reduced, but the minimum vertical fluctuation amplitude still reaches to 13.06 m/s, which reflects the strong fluctuation of typhoon wind.

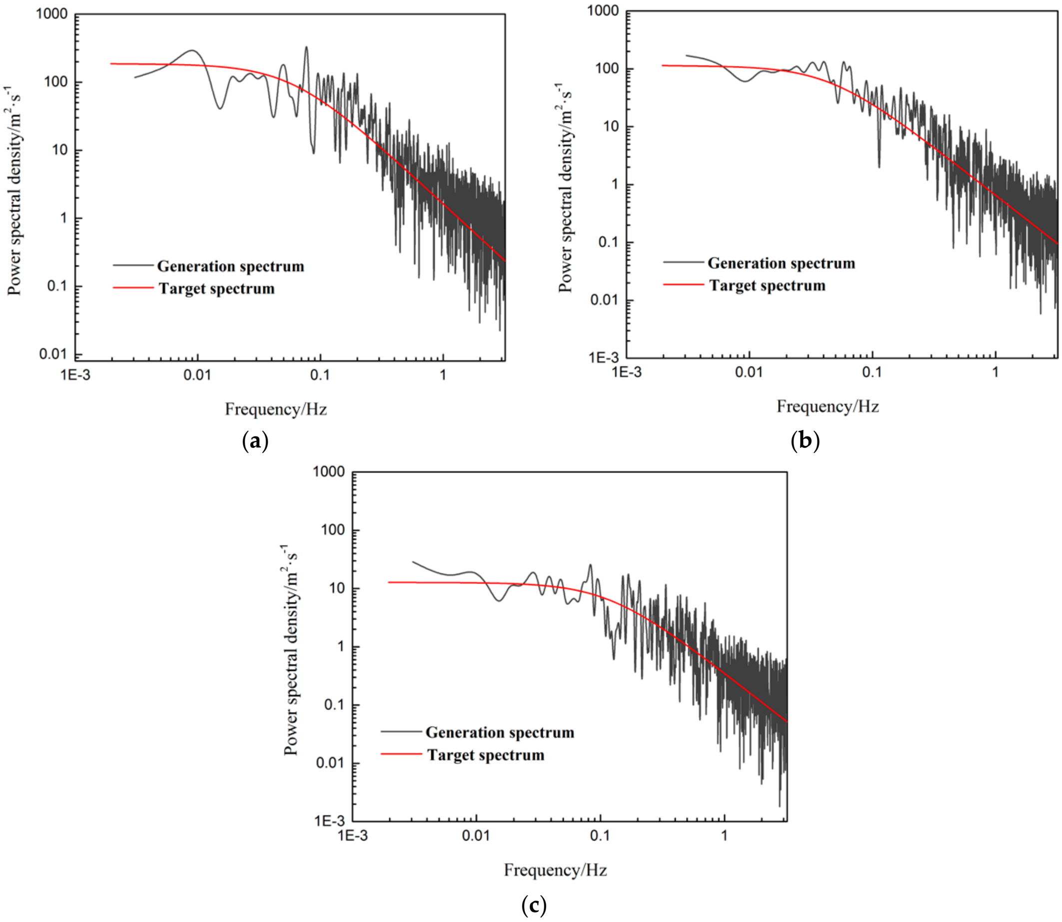

Figure 4. Comparison of the power spectrum. (**a**) *x*-direction; (**b**) *y*-direction; (**c**) *z*-direction.

Table 2. The comparison of turbulence intensity.

Direction	Measurement	Proposed	Kaimal	Von Karman
x	18%	17.7%	12.63%	15.45%
y	15%	14.3%	10.66%	12.36%
z	7%	5.8%	5.89%	7.87%

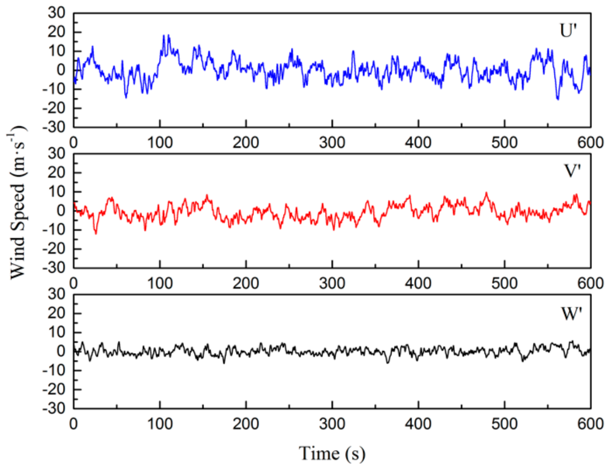

Figure 5. Fluctuating wind speed at hub height.

3.3. Analysis of Aeroelastic Response

Figure 6 shows the maximum tip displacements of three blades in the direction of the flap at yaw angles of 0, 30, 60, 90, 120, 150 and 180 degrees under typhoon. The height of blade 1 is the highest, which means that the wind speed was higher, so the total vibration of blade 1 is significantly more intense than that of the other blades. Since the yaw angle is defined as the left side of the inflow axis is positive (Figure 3), there is a positive superposition between aerodynamic and inertial load of blade 3. On the contrary, the aerodynamic and inertial loads on the blade 2 are partially offset to each other, resulting in a weakened load on the blade, and the overall vibration is slightly lower than that of blade 3. It should be noticed that, influenced by extreme fluctuating wind speed of typhoon and the combined force of lift and drag, the blade displacement reaches a maximum at this angle of attack, and the maximum displacement of the blade tip reaches 15.79 m at yaw angle of 30 degrees. As a result, it may lead to serious safety hazards of blade yaw angle of 30 degrees caused by large ultimate loads.

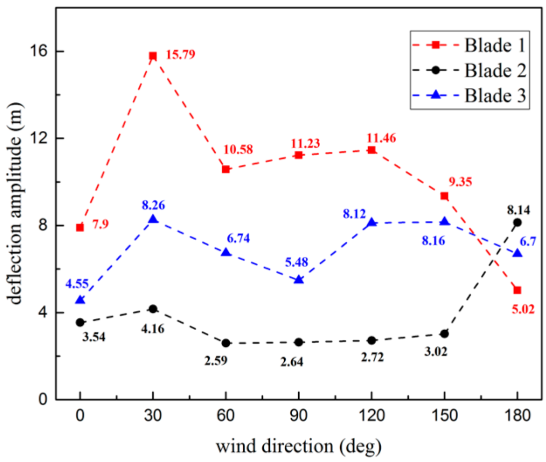

Figure 6. Comparison of the maximum tip displacement.

In order to illustrate the relationship between the ultimate design loads and the response loads under typhoon, we calculate the ultimate design loads of the blade and tower of the 6 MW wind turbine according to GL2010 standards. In addition, the dynamic loads in 10 min under different inflow conditions in the direction of the flap are also studied, and the maximum/minimum values are compared with the ultimate design loads. Figure 7 shows the comparison of the flap bending moments at the root of three blades, in which the negative value represents the direction, the red and blue curves are the maximum and minimum, respectively, and the dashed line is the ultimate design load. From the series of curves, the maximum bending moment appears at yaw angle of the 30 degrees of blade 1, and the maximum value is 2.24×10^7 Nm, which reached 71.5% of the ultimate design value according to GL2010 standards, and the minimum value is -1.17×10^7 Nm (the negative sign indicates that the direction of flapwise moment is negative), occurring at blade 3 at the inflow angle of the 30 degrees. The results show that the loads on the blades of wind turbines did not exceed the ultimate value, but the average wind speed of the typhoon simulated in this paper is only 40 m/s, far less than the ultimate wind speed of 70 m/s in the specification, and the maximum load is very close to the ultimate value.

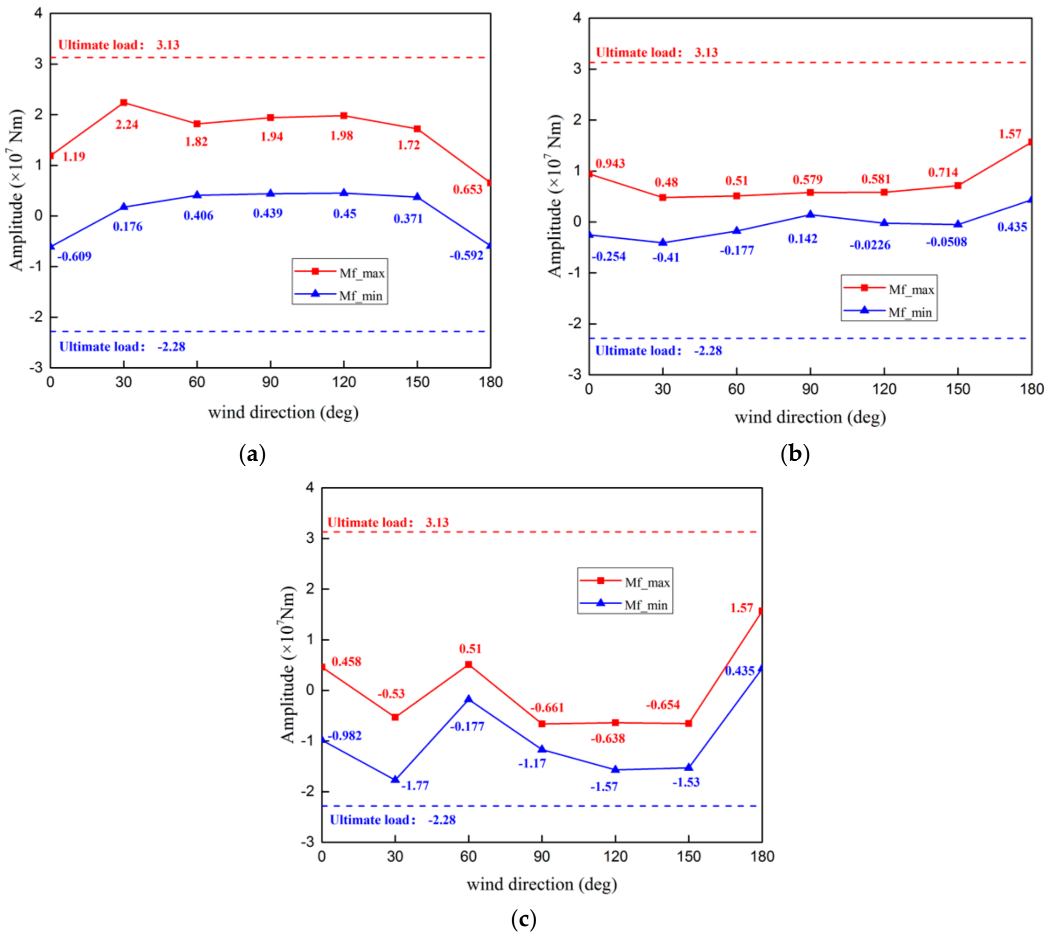

Figure 7. Flap bending moment of blade root. (**a**) Blade 1; (**b**) Blade 2; (**c**) Blade 3.

The dynamic response of the tower under the typhoon is also analyzed. Figures 8 and 9 show the results of the load on the top of the tower and the ultimate design values under different inflow conditions. When the inflow yaw angle is 120 degrees, the minimum load in the *y*-direction exceeds the design extreme value of the model. When the inflow angle is 30 degrees, it is very close to the design ultimate value. Figure 10 shows the load variations in the *y*-direction within ten minutes under six yaw inflow angles. When the inflow angle is 30 degrees and 120 degrees, respectively, the amplitude of vibration load is higher than other conditions, which means that more vibration energy is included in these cases. The above results show that, if the typhoon enters the flow at these two yaw angles, and if the yaw system does not adjust in time, the tower could be damaged.

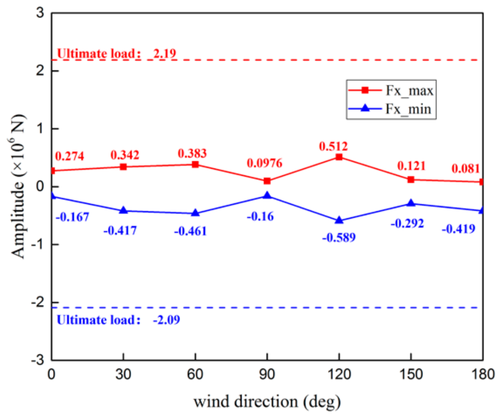

Figure 8. Fx of tower.

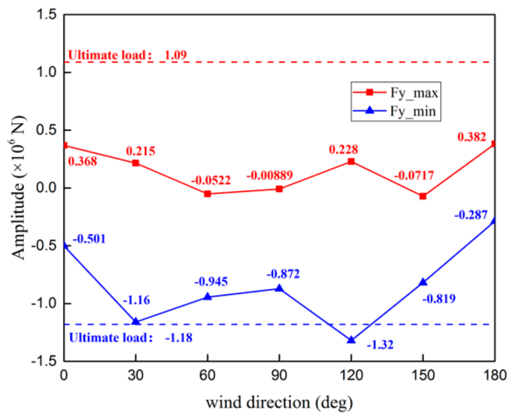

Figure 9. Fy of tower.

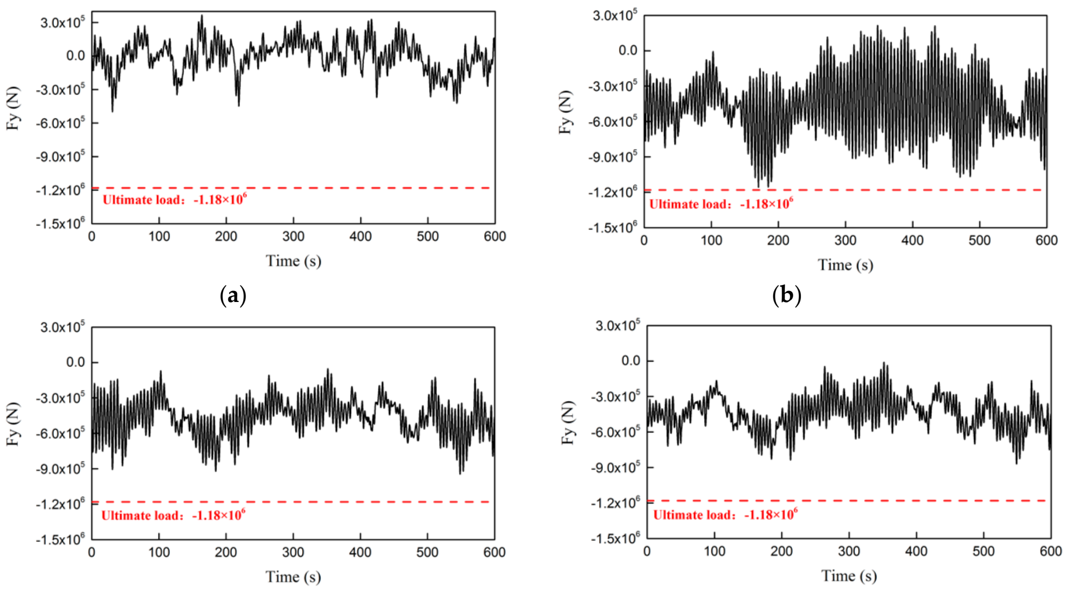

Figure 10. *Cont.*

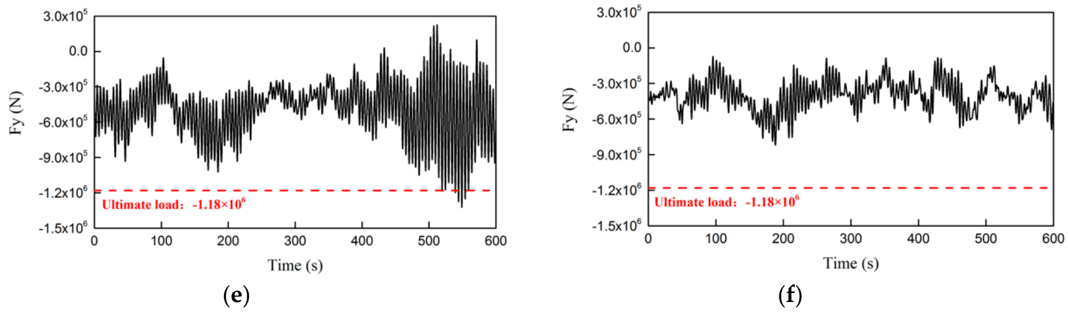

Figure 10. Variation of Fy in ten minutes. (**a**) Inflow of 0°; (**b**) Inflow of 30°; (**c**) Inflow of 60°; (**d**) Inflow of 90°; (**e**) Inflow of 120°; (**f**) Inflow of 150°.

The above results reveal that the inflow yaw angle has a significant effect on the blades and tower of the wind turbine. In order to study whether such effect is universal, a 2 MW wind turbine which is widely used at present is also modeled and calculated. The model is also a three-blade horizontal axis wind turbine whose rotor diameter is 93 m and the height of tower is 78 m. The results of 6 MW simulation show that blade 1 vibrates more intensely than other blades, and the vibration of the tower is more severe in the y-direction. Therefore, Table 3 gives the maximum tip displacement of blade 1 and the distribution of ultimate loads of the tower in the y-direction under different inflow angles of the 2 MW model. The results show that there is a significant effect on the vibration of wind turbine when the inflow yaw angle changes. The blade displacement reaches a maximum at the inflow yaw angle of 30 degrees, and the vibration amplitude of the tower in the y-direction is higher than that in other cases when the yaw angle is 30 degrees and 120 degrees, which are similar to those of the 6 MW wind turbine.

Table 3. Aeroelastic responses of 2 MW wind turbine at different yaw inflow angles of the typhoon.

Inflow Yaw Angle (Deg)	0	30	60	90	120	150	180
Deflection Amplitude of Blade 1 (m)	4.16	5.99	5.31	5.31	4.95	4.5	2.61
Fy Maximum of Tower (×105N)	2.81	7.38	2.31	2.27	7.09	4.54	2.74
Fy Minimum of Tower (×105N)	−3.48	−5.05	−5.33	−4.24	−4.61	−3.75	−2.38

In order to further study the particularity of the typhoon and its influence on the structure of wind turbine, the modal decomposition of the fluctuating wind speed is carried out in the frequency domain, and the instantaneous frequency of the intrinsic mode is obtained by the Hilbert-Huang transformation (HHT). The HHT methodclearly shows the frequency of structural response variation with time [43]. In practice, the range about structural frequency which is greatly affected by the fluctuating wind is between 0.1 Hz and 1 Hz. Figure 11 shows the instantaneous frequency in the three kinds of the fluctuating winds simulated by the different power spectrums which are located among the above frequency range. The black curve is the second order instantaneous frequency and red is the third order instantaneous frequency. The second order instantaneous frequencies in Figure 11a,b fluctuate sharply between 0.1 to 0.5 Hz, while most of the second order peak frequencies in Figure 10c are concentrated between 0.2 to 0.3 Hz. Table 1 shows that the first natural frequencies of the wind turbine blades and the towers are observed in this range, so the energy of typhoons can be more easily resonant with the structure. According to the third-order instantaneous frequency, it is found that the peak of Figure 11a changes very slightly, but there are obvious abrupt changes in Figure 11b,c. These differences show the non-stationary characteristics of the typhoon.

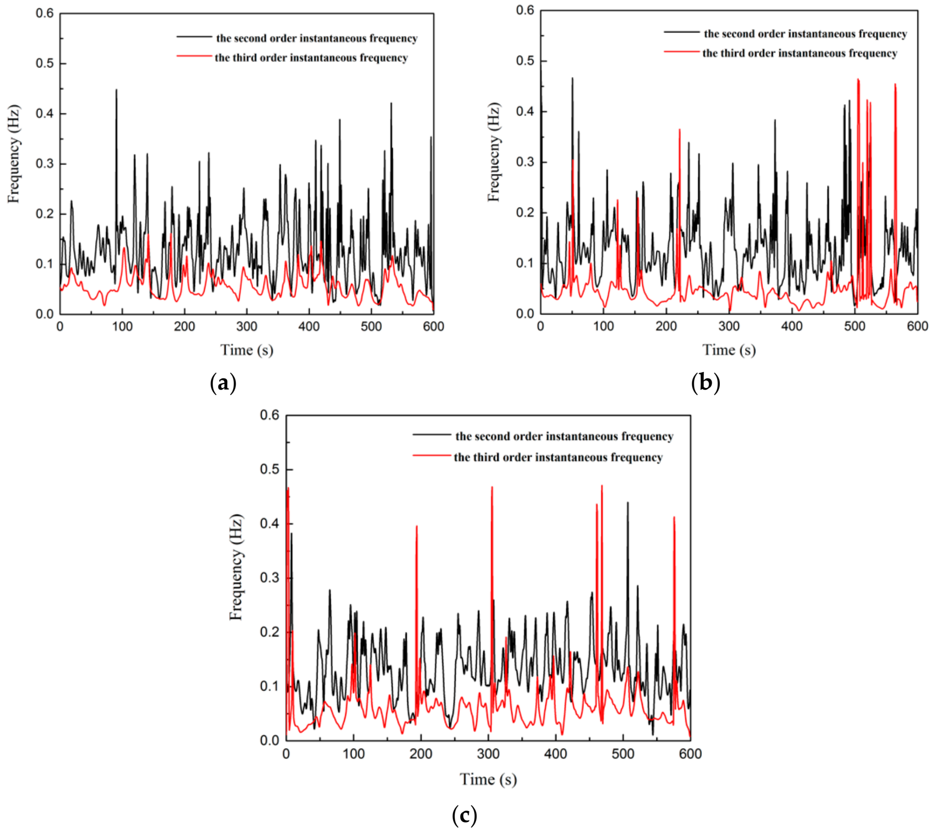

Figure 11. Comparison of the instantaneous frequencies. (**a**) simulation by Kaimal spectrum; (**b**) simulation by Von Karman spectrum; (**c**) simulation by measured spectrum.

4. Conclusions

In the present work, the random fluctuating wind with typhoon characteristics is simulated by coupling the measured data of the typhoon and inverse Fourier transformation. Based on the beam theory, a 6 MW wind turbine model is constructed to study its aeroelastic response in typhoon conditions. The aerodynamic loads and aeroelastic responses are calculated using the GH-Bladed software. A new method for calculating the dynamic responses of wind turbines under typhoon is established. The characteristics of the typhoon and the response of wind turbine at different yaw angles are analyzed. The conclusions are as follows:

1. By analyzing the power spectrum and turbulence intensity of the simulated typhoon, it is found that the characteristics are similar to the measured results. Therefore, it can be considered that the simulated wind can represent the real-time fluctuating typhoon wind and establish the calculating reliability of the wind turbine response.
2. The typhoon is simulated based on the measured spectrum and its energy mainly concentrates in the low frequency region, which is close to the natural frequency of wind turbines and it is easy to resonate with the structural coupling. There are more abrupt changes in the higher order instantaneous frequency, which reflects the non-stationary characteristics of typhoons.
3. There are significant differences in the response characteristics of wind turbines at different yaw inflow angles. Especially when the inflow angle is 30 degrees, the blade exhibits the greatest load and shows the most violent vibration; when the yaw angle is 120 degrees, the extreme load of the tower exceeds the design ultimate value obtained according to the specification. The vibration energy of the tower is much higher than that of the other working conditions when the yaw angle is 30 degrees and 120 degrees. The simulation analysis of different sizes of wind turbine models

shows that the vibration changes similarly under different inflow yaw angles, which indicates the universality of the influence of inflow yaw angles on the aeroelastic responses of wind turbines.

In this paper, the dynamic response of wind turbines in the eyewall region of typhoon is studied with the measured data. In the future, the fluctuating wind of typhoons with different wind levels and different distances from the wind eye will be simulated systematically, and the vibration characteristics and flutter instability of wind turbines in extreme weather conditions will be studied in detail. The Weather Research and Forecasting Model (WRF) for typhoon simulation and nonlinear methods for aeroelastic analysis should be taken into account for the accuracy improvements.

Author Contributions: R.H. was responsible for simulations and paper writing, L.W. and Z.G. checked the measured data and advised simulation methods, T.W. and J.W. helped analyze results.

Funding: This work was funded by the National Nature Science Foundation (Grant No. 51506089) and the Priority Academic Program Development of Jiangsu Higher Education Institutions.

Conflicts of Interest: The authors declare no conflict of interest.

References

1. Li, Q.S.; Li, X.; He, Y.; Yi, J. Observation of wind fields over different terrains and wind effects on a super-tall building during a severe typhoon and verification of wind tunnel predictions. *J. Wind Eng. Ind. Aerodyn.* **2017**, *162*, 73–84. [CrossRef]
2. Hazelton, A.T.; Rogers, R.F.; Hart, R.E. Analyzing Simulated Convective Bursts in Two Atlantic Hurricanes. *Mon. Weather Rev.* **2017**, *145*, 3073–3094. [CrossRef]
3. Kepert, J.D. Time and space scales in the tropical cyclone boundary layer and the location of the eyewall updraft. *J. Atmos. Sci.* **2017**, *74*, 3305–3323. [CrossRef]
4. Williams, G.J., Jr. The thermodynamic evolution of the hurricane boundary layer during eyewall replacement cycles. *Meteorol. Atmos. Phys.* **2017**, *129*, 611–627. [CrossRef]
5. Liu, D.; Song, L.; Li, G. Study on Wind Profile of Typhoon HAGUPIT Using Wind Observed Tower and Wind Profile Radar Measurements. *J. Trop. Meteorol.* **2011**, *27*, 317–326.
6. Song, L.; Pang, J.; Jiang, C. Measurement and Analysis of Turbulence Characteristics of Typhoon "Parrot". *J. Sci. Sin. Technol.* **2010**, *40*, 1409–1419.
7. Glauert, H. *Airplane Propellers*; Dover Publications: New York, NY, USA, 1963.
8. Prandtl, L.; Betz, A. *Vier Abhandlungen zur Hydrodynamik und Aerodynamik*; Göttinger Nachr.: Göttingen, Germany, 1927; pp. 88–92.
9. Gupta, S. *Development of a Time-Accurate Viscous Lagrangian Vortex Wake Model for Wind Turbine Applications*; University of Maryland: College Park, MD, USA, 2006.
10. Saverin, J.; Peukert, J.; Marten, D.; Pechlivanoglou, G.; Paschereit, C.O.; Greenblatt, D. Aeroelastic simulation of multi-MW wind turbines using a free vortex model coupled to a geometrically exact beam model. *J. Phys. Conf. Ser.* **2016**, *753*, 082015. [CrossRef]
11. Li, Y.; Paik, K.J.; Xing, T.; Carrica, P.M. Dynamic overset CFD simulations of wind turbine aerodynamics. *Renew. Energy* **2012**, *37*, 285–298. [CrossRef]
12. Calaf, M.; Meneveau, C.; Meyers, J. Large eddy simulation study of fully developed wind-turbine array boundary layers. *Phys. Fluids* **2010**, *22*, 46–56. [CrossRef]
13. Cai, G.P.; Hong, J.Z.; Yang, S.X. Dynamic analysis of a flexible hub-beam system with tip mass. *Mech. Res. Commun.* **2005**, *32*, 173–190. [CrossRef]
14. Gao, Y.W.; Li, C.; Cheng, X. Research on foundation response of a tri-floater offshore wind turbine. *Conf. Ser. Mater. Sci. Eng.* **2013**, *52*, 66–71. [CrossRef]
15. Rezaei, M.M.; Behzad, M.; Haddadpour, H.; Moradi, H. Aeroelastic analysis of a rotating wind turbine blade using a geometrically exact formulation. *Nonlinear Dyn.* **2017**, *89*, 2367–2392. [CrossRef]
16. Ho, J.Y.L. Direct Path Method for Flexible Multibody Spacecraft Dynamics. *J. Spacecr. Rocket.* **2012**, *14*, 102–110. [CrossRef]
17. Zhao, X.; Maißer, P.; Wu, J. A new multibody modelling methodology for wind turbine structures using a cardanic joint beam element. *Renew. Energy* **2007**, *32*, 532–546. [CrossRef]

18. Wang, L.; Wang, T.; Wu, J.; Chen, G. Multi-objective differential evolution optimization based on uniform decomposition for wind turbine blade design. *Energy* **2017**, *120*, 346–361. [CrossRef]
19. Han, T.; McCann, G.; Mücke, T.A.; Freudenreich, K. How can a wind turbine survive in tropical cyclone? *Renew. Energy* **2014**, *70*, 3–10. [CrossRef]
20. Xiao, C.; Li, C. Failure investigation on a coastal wind farm damaged by super typhoon: A forensic engineering study. *J. Wind Eng. Ind. Aerodyn.* **2015**, *147*, 132–142.
21. Chen, X.; Xu, J. Structural failure analysis of wind turbines impacted by super typhoon Usagi. *Eng. Fail. Anal.* **2016**, *36*, 391–404. [CrossRef]
22. Chen, X. Structural integrity of wind turbines impacted by tropical cyclones: A case study from China. *J. Phys. Conf. Ser.* **2016**, *753*, 1–12. [CrossRef]
23. Zhang, Z.; Li, J.; Ping, Z. Failure Analysis of Large-Scale Wind Power Structure under Simulated Typhoon. *Math. Probl. Eng.* **2003**, *4*, 30–32. [CrossRef]
24. Dai, K.; Sheng, C.; Zhao, Z. Nonlinear response history analysis and collapse mode study of a wind turbine tower subjected to tropical cyclonic winds. *Wind Struct.* **2017**, *25*, 79–100.
25. Lian, J.; Jia, Y.; Wang, H.; Liu, F. Numerical Study of the Aerodynamic Loads on Offshore Wind Turbines under Typhoon with Full Wind Direction. *Energies* **2016**, *9*, 613. [CrossRef]
26. Fang, P.; Zhao, B.; Zeng, Z.; Yu, H.; Lei, X.; Tan, J. Effects of Wind Direction on Variations in Friction Velocity WithWind Speed Under Conditions of Strong Onshore Wind. *J. Geophys. Res. Atmos.* **2018**, *123*, 7340–7353.
27. Dai, L.; Zhou, Q.; Zhang, Y.; Yao, S.; Kang, S.; Wang, X. Analysis of wind turbine blades aeroelastic performance under yaw conditions. *J. Wind Eng. Ind. Aerodyn.* **2017**, *171*, 273–287. [CrossRef]
28. Wen, B.; Tian, X.; Dong, X.; Peng, Z.; Zhang, W.; Wei, K. A numerical study on the angle of attack to the blade of a horizontal-axis offshore floating wind turbine under static and dynamic yawed conditions. *Energy* **2019**, *168*, 1138–1156. [CrossRef]
29. Chen, J.; Shen, X.; Zhu, X.; Du, Z. Influence of wake asymmetry on wind turbine blade aerodynamic and aeroelastic performance in shear/yawed wind. *J. Renew. Sustain. Energy* **2018**, *10*, 053309. [CrossRef]
30. Chen, X.M.; Kang, S. Numerical Simulation of the Unsteady Aerodynamic of Wind Turbine under Yaw Condition. *Adv. Mater. Res.* **2015**, *1070*, 1883–1887. [CrossRef]
31. Yin, L.L.; Lo, K.H.; Wang, S.S. Effects of Blade Pitch, Rotor Yaw, and Wind–Wave Misalignment on a Large Offshore Wind Turbine Dynamics in Western Gulf of Mexico Shallow Water in 100-Year Return Hurricane. *J. Offshore Mech. Arct. Eng.* **2017**, *139*, 011901. [CrossRef]
32. Ebrahimi, A.; Sekandari, M. Transient response of the flexible blade of horizontal-axis wind turbines in wind gusts and rapid yaw changes. *Energy* **2018**, *145*, 261–275. [CrossRef]
33. Dong, X.; Lian, J.; Wang, H.; Yu, T.; Zhao, Y. Structural vibration monitoring and operational modal analysis of offshore wind turbine structure. *Ocean Eng.* **2018**, *150*, 280–297. [CrossRef]
34. Bassett, K.; Carriveau, R.; Ting, D.S. Ting1 Vibration response of a 2.3 MW wind turbine to yaw motion and shut down events. *Wind Energy* **2011**, *14*, 939–952. [CrossRef]
35. Uzunoglu, E.; Soares, C.G. Yaw motion of floating wind turbine platforms induced by pitch actuator fault in storm conditions. *Renew. Energy* **2019**, *134*, 1056–1070. [CrossRef]
36. Song, L.; Chen, W.; Wang, B.; Zhi, S.; Liu, A. Characteristics of wind profiles in the land falling typhoon boundary layer. *J. Wind Eng. Ind. Aerodyn.* **2016**, *49*, 77–88. [CrossRef]
37. Tony, B.; David, S.; Nick, J.; Ervin, B. *Wind Energy*; John Wiley & Sons, Ltd.: Hoboken, NJ, USA, 2001.
38. Li, L.; Xiao, Y.; Kareem, A.; Song, L.; Qin, P. Modeling typhoon wind power spectra near sea surface basedon measurements in the South China sea. *J. Wind Eng. Ind. Aerodyn.* **2012**, *104*, 565–576. [CrossRef]
39. Hu, S.; Song, L.; Li, Q. Monitoring of typhoons in surface boundary layer and analysis of wind turbulence characteristics. *J. Build. Struct.* **2011**, *32*, 1–8.
40. Rossi, R.; Lazzari, M.; Vitaliani, R. Wind field simulation for structural engineering purposes. *Int. J. Numer. Methods Eng.* **2004**, *61*, 738–763. [CrossRef]
41. Shiotani, M.; Avai, H. Lateral Structures of Gusts of High Winds. In Proceedings of the International Research Seminar on Wind Effects on Buildings and Structures, Ottawa, ON, Canada, 11–15 September 1967; pp. 535–555.

42. Bossanyi, E.A. *GH Bladed Theory Manual*; Garrad Hassan; Garrad Hassan and Partners: Bristol, UK, 2009; pp. 13–19.
43. Huang, N.E.; Shen, Z.; Long, S.R. The Empirical Mode Decomposition and the Hilbert Spectrum for Nonlinear and non-Stationary Time Series Analysis. *Math. Phys. Eng. Sci.* **1998**, *454*, 903–995. [CrossRef]